Electronic Supplementary Information (ESI)

3D Architecture Constructed via Confined Growth of MoS_2 Nanosheets in Nanoporous Carbon Derived from Metal-Organic Frameworks for Efficient Hydrogen Production

Yun Liu,‡[abcd] Xiaoli Zhou,‡[abcd] Tao Ding[abcd] Chunde Wang[abcd] and Qing Yang*[abcd]

[a] Hefei National Laboratory of Physical Sciences at the Microscale, University of Science and Technology of China (USTC), Hefei 230026, Anhui, P. R. China.

[b] Department of Chemistry, USTC, Hefei 230026, Anhui, P. R. China.

[c] Laboratory of Nanomaterials for Energy Conversion, USTC, Hefei 230026, Anhui, P. R. China.

[d] Synergetic Innovation Center of Quantum Information & Quantum Physics, USTC, Hefei 230026, P. R. China.

* Corresponding author. E-mail: qyoung@ustc.edu.cn; Fax: +86-551-63606266; Tel: +86-551-63600243.

‡ These authors contributed equally to this work

1. Experimental section:

Materials. All reagents were used directly without further purification.

Synthesis of MoS_2/3D-NPC composite. The 3D-NPC was prepared via Ming Hu method.[S1, S2] To prepare MoS_2/3D-NPC composites, 20 mg $(NH_4)_2MoS_4$ (Sigma Aldrich) and 10 mg 3D-NPC was added in 10 mL DMF. The mixture was stirred at room temperature for approximately 12 h until a homogeneous solution was achieved. After that, 0.1 mL $N_2H_4 \bullet H_2O$ was added into the suspension. After stirring for another 30 min, the mixed solution was transferred into a 20 mL Teflon-lined autoclave, which was sealed and heated in an oven at 200 °C for 35 min, 1 h, 5 h and 10 h with no intentional control of ramping or cooling rate. Products were collected by centrifugation at 10000 rpm for 4 min, washed with DI water and recollected by centrifugation. The washing step was repeated for at least 4 times to ensure that ions and possible remnants were removed. Finally, the product was dried 12 h at 70 ^oC in an oven.

Synthesis of free MoS_2 nanoparticles. The synthetic procedure of free MoS_2 nanoparticles is the same as the one for preparing the MoS_2/3D-NPC composites except for that 3D-NPC was removed from the synthetic procedure.

Electrochemical measurements. 4 mg of catalyst and 40 uL of 5 wt% Nafion solution (Sigma Aldrich) were dispersed in 1 mL of 4:1 v/v water/DMF by sonicating at least 30 min to form a homogeneous solution. Then 5 μL of the catalyst ink (containing 20 μg of catalyst) was loaded onto a glassy carbon electrode of 3 mm in diameter (loading ~ 0.285 mg cm^{-2}). Linear sweep voltammetry (using the CHI660E Instruments) with scan rate of 5 mV s^{-1} was conducted in Ar-saturated 0.5M H_2SO_4 using Ag/AgCl (in saturated KCl solution) electrode as the reference electrode, a platinum electrode as the counter electrode and the glassy carbon electrode as the working electrode. The electrochemical impedance spectroscopy measurement was performed were carried out in the same configuration at overpotential η = 200 mV from 10^6 – 0.02 Hz at the amplitude of 5 mV. For the stability tests, the potential of the electrodes cycled between a potential range from -0.25 to 0.2V vs RHE at a sweep rate of 50 mV s^{-1}. At the end of the cycling experiment, the polarization curve was obtained with a sweep rate of 5 mV s^{-1}. The current density was normalized by geometric electrode area (0.07 cm^2). The potentials reported in our work were referenced to the reversible hydrogen electrode (RHE): $E_{RHE} = E_{Ag/AgCl} + 0.059 \times pH + 0.1981$ (in this test, pH=0.04). All data were reported with iR compensation.

Characterization. The products were characterized using X-ray powder diffraction (XRD, performed on a Philips X'pert PRO X-ray diffractometer, Cu Kα, λ = 1.54182 Å), scanning electron microscope (SEM, JSM-6700F). The high resolution TEM (HRTEM), high-angle annular dark-field scanning transmission electron microscopy (HAADF-STEM) and corresponding energy-dispersive spectroscopic (EDS) mapping analyses were performed on a JEOL JEM-ARF200F TEM/STEM with a spherical aberration corrector. X-ray photoelectron spectra (XPS) were acquired on an ESCALAB MK II with Mg Kα as the excitation source. The nitrogen absorption/desorption isotherms were obtained at 77 K on an ASAP 2020 accelerated surface area and porosimetry instrument (Micromeritics). The electrical measurements were carried out using a

Keithley 4200-SCS Semiconductor characterization system by a two probe configuration.

2. Supplementary Figures

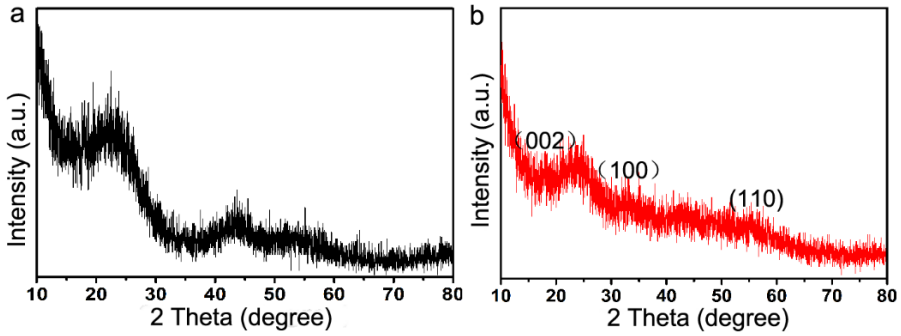

Fig. S1. XRD patterns of (a) 3D-NPC, and (b) MoS_2/3D-NPC composites using DMF as the solvent with reaction time for 1h.

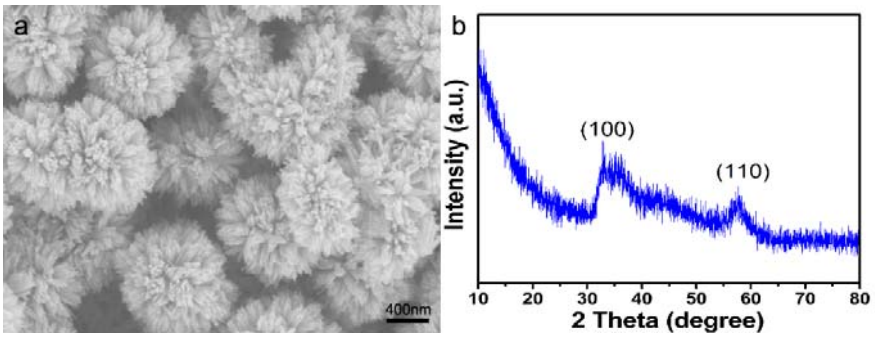

Fig. S2. (a) SEM image and (b) XRD pattern of the MoS_2 nanoparticles obtained by using DMF as the solvent with reaction time for 1h.

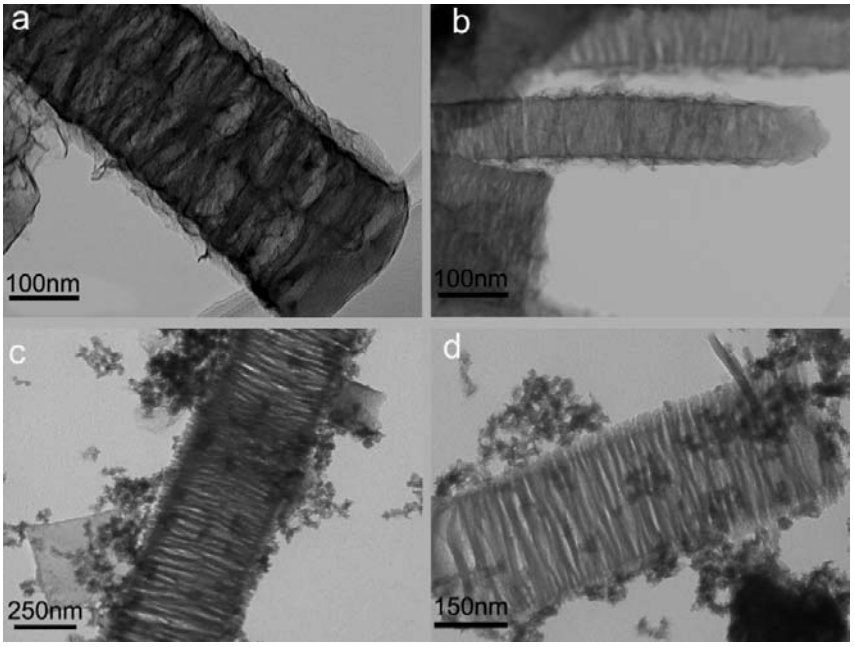

Fig. S3. (a) Additional TEM image of the as-obtained MoS_2/3D-NPC composites in the media of

DMF, and (b) TEM image of the MoS_2/3D-NPC composites after repeated washing and ultrasonication cycles. TEM images of the samples by replacing the DMF with (c) water and (d) iso-propanol as solvent. All the reaction time was 1h.

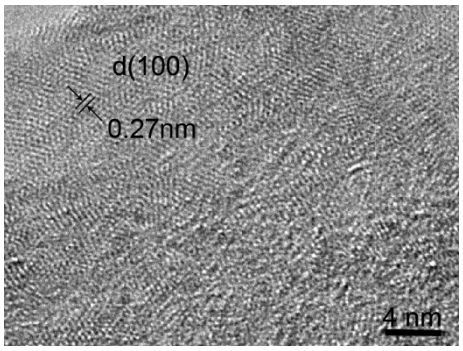

Fig. S4. HRTEM image of the MoS_2/3D-NPC composites, showing low crystallinity of MoS_2 nanosheets.

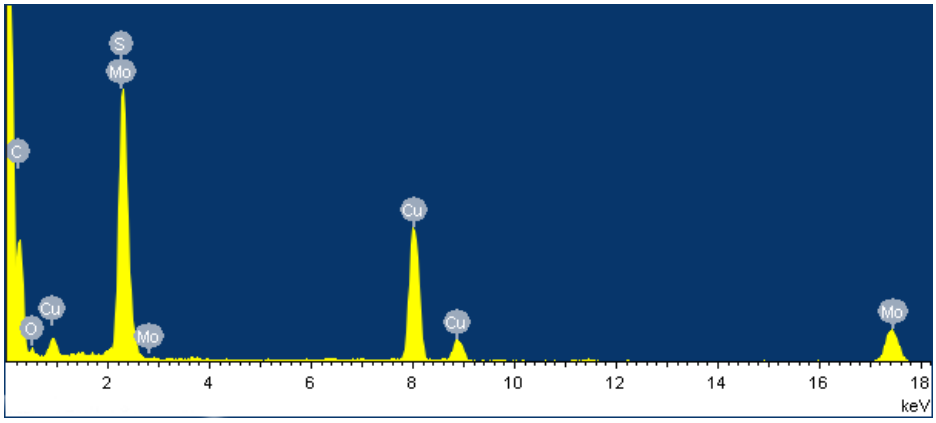

Fig. S5. EDX spectra of the MoS_2/3D-NPC composites. The signal of Cu arises from the TEM grid.

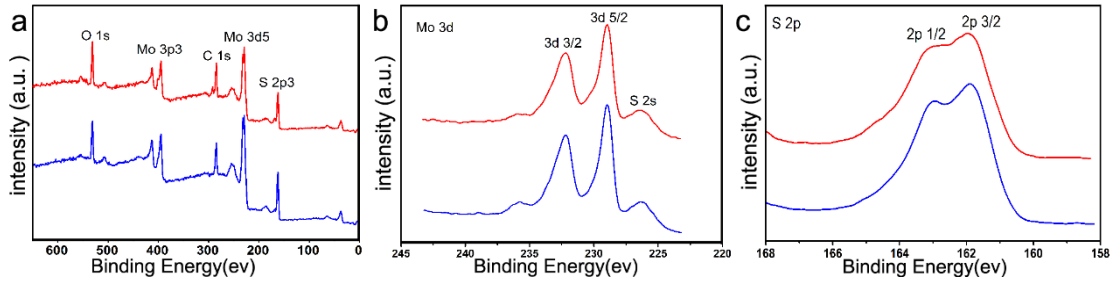

Fig. S6. (a) XPS survey spectra of the MoS_2/3D-NPC composites and pure MoS_2 nanoparticles. (b) - (d) high-resolution XPS spectra of the Mo 3d and S 2p for the MoS_2/3D-NPC composites (red lines) and pure MoS_2 nanoparticles (blue lines).

We have compared Mo 3d and S 2p XPS spectra of the as-synthesized MoS_2/3D-NPC composites (red line) with pure MoS_2 nanoparticles (blue line). As shown in Figure S10, no obvious shift is observed between the MoS_2/3D-NPC composites and pure MoS_2 nanoparticles. For the MoS_2/3D-NPC composites synthesized in our experimental condition, the interaction

between MoS_2 nanosheets and 3D-NPC is not strong enough to influence the valence states of the elements. Moreover, according to the literatures of other MoS_2-based hybrids, we found that there were no obvious changes of valence states of the elements in previous reports, but the hybrids system showed highly improved performance for HER.

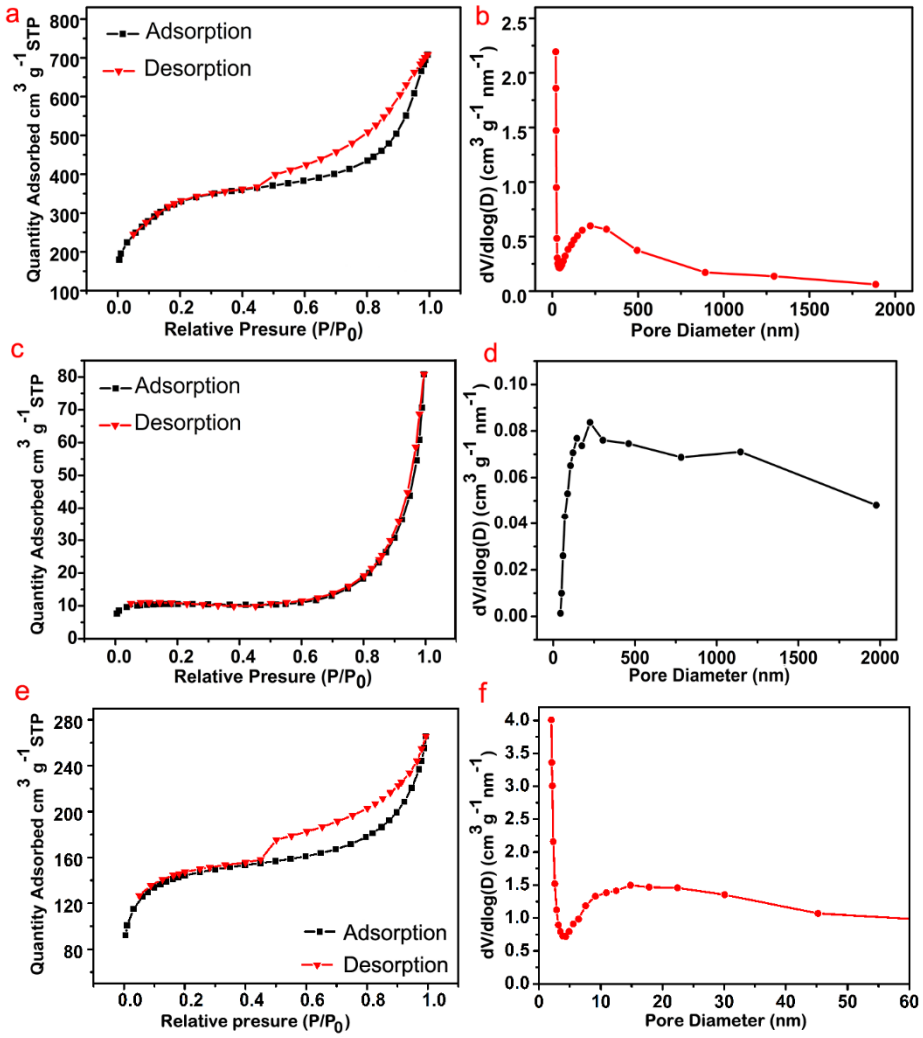

Fig. S7. (a) N_2 adsorption/desorption isotherms and (b) pore size distribution of pure 3D-NPC. (c) N_2 adsorption/desorption isotherms and (d) pore size distribution of pure MoS_2 nanoparticles. (e) N_2 adsorption/desorption isotherms and (f) pore size distribution of the MoS_2/3D-NPC composites. All data are obtained by using the BJH method.

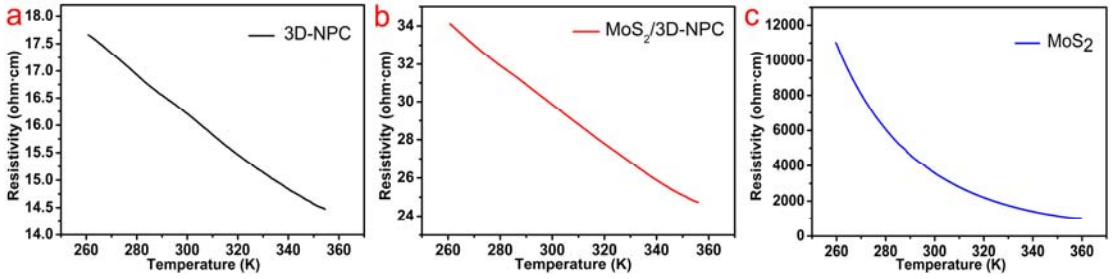

Fig. S8. Temperature-dependent electrical resistivity of (a) the 3D-NPC, (b) the MoS_2/3D-NPC composites, and (c) the MoS_2 nanoparticles, respectively.

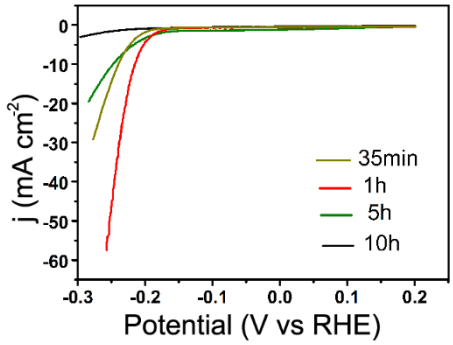

Fig. S9. Polarization curves of the MoS_2/3D-NPC composites with reaction time for 35min, 1h, 5h and 10h, respectively.

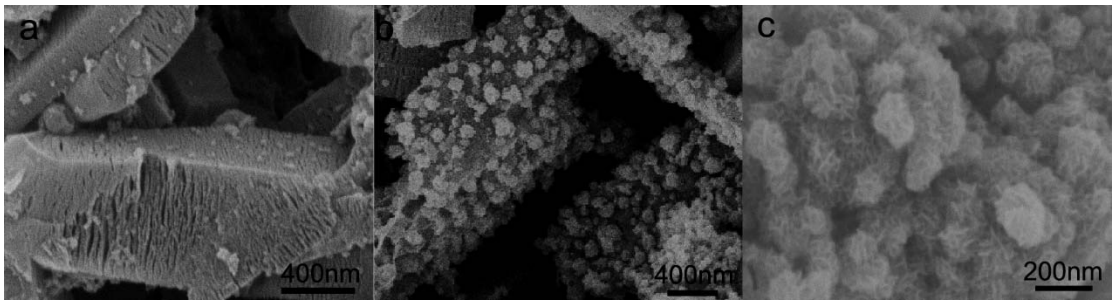

Fig. S10. SEM images of the MoS_2/3D-NPC composite obtained after (a) 35min, (b) 5h, and (c) 10h, respectively.

References

S1. Comotti, A.; Bracco, S.; Sozzani, P.; Horike, S.; Matsuda, R.; Chen, J.; Takata, M.; Kubota, Y.; Kitagawa, S. *J. Am. Chem. Soc.* 2008, **130**, 13664-13672.

S2. Hu, M.; Reboul, J.; Furukawa, S.; Torad, N. L.; Ji, Q.; Srinivasu, P.; Ariga, K.; Kitagawa, S.; Yamauchi, Y. *J. Am. Chem. Soc.* 2012, **134,** 2864-2867.